Eur. Phys. J. A **27**, 129–136 (2006)
DOI 10.1140/epja/i2005-10258-0

THE EUROPEAN PHYSICAL JOURNAL A

Beta decay of the proton-rich nuclei ^{102}Sn and ^{104}Sn

M. Karny[1,a], L. Batist[2], A. Banu[3], F. Becker[3], A. Blazhev[3,4], B.A. Brown[5], W. Brüchle[3], J. Döring[3], T. Faestermann[6], M. Górska[3], H. Grawe[3], Z. Janas[1], A. Jungclaus[7], M. Kavatsyuk[3,8], O. Kavatsyuk[3,8], R. Kirchner[3], M. La Commara[9], S. Mandal[3], C. Mazzocchi[3], K. Miernik[1], I. Mukha[3], S. Muralithar[3,10], C. Plettner[3], A. Płochocki[1], E. Roeckl[3], M. Romoli[9], K. Rykaczewski[11], M. Schädel[3], K. Schmidt[12], R. Schwengner[13], and J. Żylicz[1]

[1] Institute of Experimental Physics, University of Warsaw, Poland
[2] St. Petersburg Nuclear Physics Institute, Russia
[3] Gesellschaft für Schwerionenforschung, Darmstadt, Germany
[4] University of Sofia, Bulgaria
[5] NSCL, Department of Physics and Astronomy, Michigan State University, USA
[6] Technische Universität München, Germany
[7] Departamento de Fisica Teórica, Universidad Autonoma de Madrid, Spain
[8] Taras Shevchenko Kiev National University, Ukraine
[9] Dipartimento Scienze Fisiche, Università "Federico II" and INFN Napoli, Italy
[10] Nuclear Science Center, New Delhi, India
[11] Oak Ridge National Laboratory, USA
[12] Continental Teves AG & Co., Frankfurt am Main, Germany
[13] Institut für Kern- und Hadronenphysik, Forschungszentrum Rossendorf, Dresden, Germany

Received: 21 October 2005 / Revised version: 12 January 2006 /
Published online: 24 March 2006 –
Communicated by C. Signorini

Abstract. The β decays of ^{102}Sn and ^{104}Sn were studied by using high-resolution germanium detectors as well as a Total Absorption Spectrometer (TAS). For ^{104}Sn, with three new β-delayed γ-rays identified, the total Gamow-Teller strength (B_{GT}) value of 2.7(3) was obtained. For ^{102}Sn, the γ-γ coincidence data were collected for the first time, allowing us to considerably extend the decay scheme. This scheme was used to unfold the TAS data and to deduce a B_{GT} value of 4.2(8) for this decay. This result is compared to shell model predictions, yielding a hindrance factor of 3.6(7) in agreement with those obtained previously for ^{98}Cd and ^{100}In. Together with the latter two, ^{102}Sn completes the triplet of $Z \leq 50$, $N \geq 50$ nuclei with two proton holes, one proton hole and one neutron particle, and two neutron particles with respect to the doubly magic ^{100}Sn core.

PACS. 21.10.-k Properties of nuclei; nuclear energy levels – 23.40.-s Beta decay; double β decay; electron and muon capture – 23.20.Lv Gamma transitions and level energies – 27.60.+j $90 \leq A \leq 149$

1 Introduction

Beta decays of nuclei "southeast" of ^{100}Sn ($Z \leq 50$, $N \geq 50$) are characterized by large decay energies (Q_{EC}) and pure Gamow-Teller (GT) transitions transforming a $g_{9/2}$ proton to a $g_{7/2}$ neutron. These features make studies of these decays especially important to test the nuclear shell model in general and its predictions of (the quenching of) the GT strength in particular. As the half-lives of these nuclei are between a fraction of a second and a few minutes experiments using on-line mass separation are feasible. The experimentally derived quantity which can be directly compared to the theoretical predictions is the β strength function. The theoretically predicted GT strength is defined as the squared matrix element of the free $\sigma\tau$ operator acting between the wave functions of the initial (Ψ_i) and the final (Ψ_f) state:

$$B_f^{th} = \langle \Psi_f | \sigma\tau | \Psi_i \rangle^2. \quad (1)$$

B_f^{th} should be compared to the experimental value derived as

$$B_f^{exp} = \frac{6147 \text{ s}}{(g_A/g_V)^2} \cdot \frac{I_\beta}{f(Q_{EC} - E_f^*) \cdot T_{1/2}}, \quad (2)$$

where g_A and g_V are the axial-vector and vector weak-interaction coupling constants, respectively, I_β the β-decay intensity to the final level f, Q_{EC} the total decay

[a] e-mail: karny@mimuw.edu.pl

energy available, $f(Q_{EC}-E_f^*)$ the statistical rate function for the transition to the level at the excitation energy E_f^*, and $T_{1/2}$ the half-life of the decaying nucleus (in seconds). By summing eq. (2) over all final levels, one obtains the total GT strength value (B_{GT}) which is a valuable quantity for comparing theory and experiment.

Southeast of ^{100}Sn, the β decays of more than 15 isotopes have been investigated [1–13] so far, reaching from ^{96}Pd to ^{105}Sn and including, in particular, ^{98}Cd [4] and ^{100}In [10] which are the closest neighbours of ^{100}Sn whose B_{GT} values are known. These two nuclei represent two proton-hole and one proton hole/one neutron particle configurations, respectively, with reference to the ^{100}Sn core. In this paper we present data on the decay of the third isotope in this family, ^{102}Sn, which has two neutrons more than ^{100}Sn. Moreover, we describe measurements of the β decay of ^{104}Sn. The GT decay of even-even, 0^+ nuclei southeast of ^{100}Sn is expected to be dominated by the $\pi g_{9/2} \rightarrow \nu g_{7/2}$ transition and thus strongly populating 1^+ states in the odd-odd daughter nuclei.

After describing the experimental techniques in sect. 2 we shall present the results for ^{104}Sn and ^{102}Sn in sects. 3.1 and 3.2, with the discussion and summary given in sects. 4 and 5, respectively. Beta-decay studies performed at the GSI on-line mass separator on light tin isotopes have been reviewed in a recent conference contribution [14] which includes a short summary of the ^{102}Sn data presented in this work.

2 Experimental techniques

The data presented in this paper were obtained by using the GSI on-line mass separator. Two complementary techniques were used, namely, a Total Absorption Spectrometer (TAS) for a β-feeding measurement, and a high-resolution array of germanium (Ge) and silicon (Si) detectors to gather information on the ^{102}Sn $\rightarrow$ ^{102}In and ^{104}Sn $\rightarrow$ ^{104}In decay schemes.

2.1 Production and mass separation

^{104}Sn and ^{102}Sn isotopes were produced by means of fusion-evaporation reactions between a ^{58}Ni beam and a ^{50}Cr target. In the various measurements, the energy of the ^{58}Ni beam varied from 284 to 302 MeV on target, while its intensity amounted to 30 to 40 particle-nA. The ^{50}Cr target of around 3 mg/cm^2 thickness was placed close to a FEBIAD-B2 ion source [15]. The catcher for the reaction recoils, mounted inside the ion source, consisted of carbon, niobium or zirconium-oxide. The ion source was operated with the addition of CS_2 vapour and thus very selectively produced SnS^+ molecular ions [16]. A separation efficiency of about 10% [16] was achieved for ^{102}Sn and ^{104}Sn. After ionization, acceleration to 55 keV and mass separation, the ions of $A = 102 + 32$ or $A = 104 + 32$ were directed to the high-resolution setup or to the TAS. The intensity of the mass-separated beam, determined on the basis of the TAS spectra measured for β^+ and electron-capture (EC) decay, was found to be about 520 atoms/s for ^{104}Sn at a ^{58}Ni beam intensity of 40 particle-nA. A similar analysis for ^{102}Sn was impossible due to the poor statistics of the EC spectrum of this decay. In view of the strong isobaric impurities, only a less accurate evaluation was performed on the basis of the β^+ spectrum, yielding an intensity of $\approx$ 30 atoms/min for ^{102}Sn at a ^{58}Ni beam intensity of 40 particle-nA. The above rate estimates correspond to the production cross-section (averaged over 3 mg/cm^2 target thickness) of 0.6 μb and 0.5 mb for ^{102}Sn and ^{104}Sn, respectively.

2.2 High-resolution setup

For the high-resolution measurement the mass-separated beam was implanted into a transport tape in the center of the Ge-Si array. The implantation point (in vacuum) was viewed by three Si detectors (60 mm $\times$ 60 mm, 1 mm thick) which formed a prism-shaped array. Outside the vacuum chamber, an array of one Cluster, two Clover and two coaxial Ge detectors was placed. The photo-peak efficiency of the Ge array amounted to 3.9% at 1.3 MeV γ-ray energy, while the silicon array covered a solid angle of approximately 65% of 4π. Details of the Ge-Si setup can be found in ref. [17]. In order to minimize the load of the data acquisition system only β-γ and γ-γ coincidence events were stored. In the off-line analysis, the events were sorted into β-gated γ-γ matrixes. The total measurement time amounted to 76 hours for ^{102}Sn, and 3.6 hours for ^{104}Sn.

2.3 Total absorption spectrometer

The TAS [18] consists of a large NaI crystal (diameter 356 mm, length 356 mm) with the radioactive source being placed in its center. As ancillary detectors, two small Si detectors (thickness 450 μm, diameter 16 mm) are mounted above (TOP) and below (BOT) the source position. Moreover, for the detection of X-rays and low-energy γ-rays a small Ge detector (thickness 10 mm, diameter 16 mm) equipped with a thin beryllium window is placed above the TOP detector. By demanding coincidence between signals from the NaI and Si detectors, the β^+ component of the TAS spectrum can be selected, while coincidences between signals from the NaI crystal and respective X-rays detected in the Ge detector are used to select the EC decay. The GEANT3 Monte Carlo code was used to simulate TAS response functions [19] needed to reconstruct β^+ and EC spectra during the data evaluation process. Reconstruction of the experimental spectra started with creation of the response function for each particular level, based on the decay scheme deduced in high-resolution studies extended (if needed) by so-called "pseudo-levels". Sum of those response function weighted with beta-feeding gives a simulated spectrum. Further analysis used the chi-square fit of the simulated spectrum to the experimental one with β-feeding as free parameters. A more detailed description

of the analysis can be found in [6,9], while the alternative approaches to the TAS data analysis were described in [20] and recently applied in [21].

Radioactive sources for the TAS measurements were produced by implanting the mass-separated beam into a transport tape, with the resulting radioactive sources being periodically moved within 0.8 s through a differential pumping system from the collection point (in vacuum) to the center of the TAS (in air). The collection/measurement cycle was chosen to be 4.8 s/4.8 s and 32 s/128 s for ^{102}Sn and ^{104}Sn, respectively. In the case of ^{102}Sn an additional experiment with a cycle of 4.8 s/20 s was performed. The asymmetric cycles were meant for obtaining data on long-lived daughter products (*i.e.*, ^{102}In and ^{104}In, respectively) as well as other isobaric contaminants (*i.e.*, ^{102}Ag and ^{104}Ag, respectively). The total measurement time amounted to 69 hours and 20 minutes for ^{102}Sn and ^{104}Sn, respectively.

3 Results

3.1 Beta decay of ^{104}Sn

The β decay of ^{104}Sn has previously been studied [22], the latest publications being those by Barden *et al.* [23] and Szerypo *et al.* [24]. The β decay of the 0^+, 20.8(5) s ground state of ^{104}Sn was found to populate four 1^+ states in ^{104}In which de-excite to the 6^+ ground state via intermediate levels including a (3^+), 15.7(5) s isomer at 93.5 keV. Figure 1 presents the decay scheme of ^{104}Sn as presented in [24] expanded by newly observed four γ-transitions at 912.6, 1273.5, 1425.4 and 1845.8 keV as well as three levels at 1500, 1651 and 2072 keV. The coincidence relations of the new transitions as well as their energies and intensities are presented in table 1. The states at 1500, 1651 and 2072 keV have been identified on the basis of the observation of β-delayed γ-rays of 912.6, 1425.4 and 1845.8 keV as well as their coincidence relationships with the most intense β-delayed γ-ray in the ^{104}Sn decay, *i.e.* that of 133 keV. Please note an existence of two 912.6 keV transitions on fig. 1: the first (very strong) de-exciting the 1139 keV level and the second (ten times weaker) depopulating the newly introduced 1651 keV level.

Table 1. Energies (E_γ), intensities (I_γ) and coincidence relationships of the new β-delayed γ-rays assigned to the decay of ^{104}Sn. The uncertainty of the γ-ray energies amounts to about 0.5 keV.

E_γ (keV)	I_γ [a]	Energies of γ-rays in coincidence (keV)
912.6	≈ 6.7	76[b], 133, 645
1273.5	4.2	133
1425.4	2.2	133
1845.8	2.0	70[b], 133

[a] Normalized to the intensity of the 133 keV line.
[b] Not placed in the level scheme.

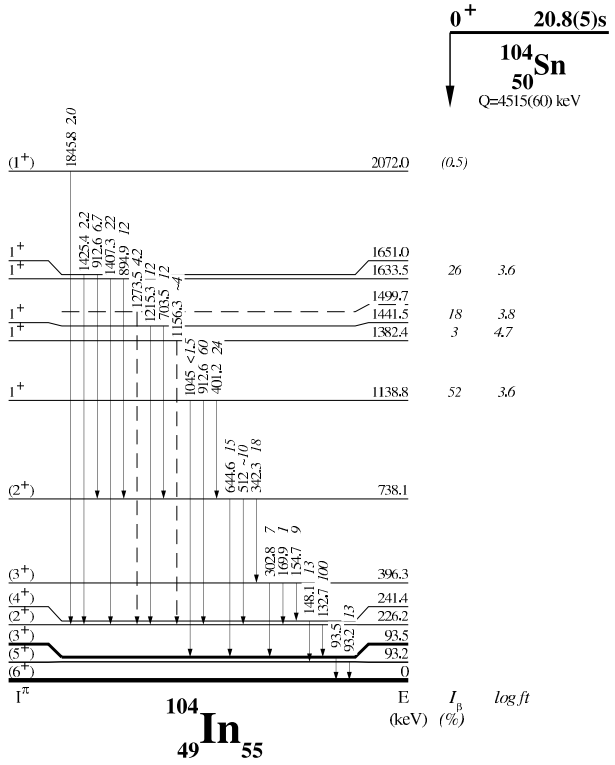

Fig. 1. ^{104}Sn decay scheme based on data from [24] and this work. The γ-ray intensities, normalized to that of the 133 keV line, represent results from [24] together with our high-resolution measurement. The β intensities (I_β) and the comparative half-lives ($\log ft$) stem from TAS data. Dashed lines indicate tentative assignments.

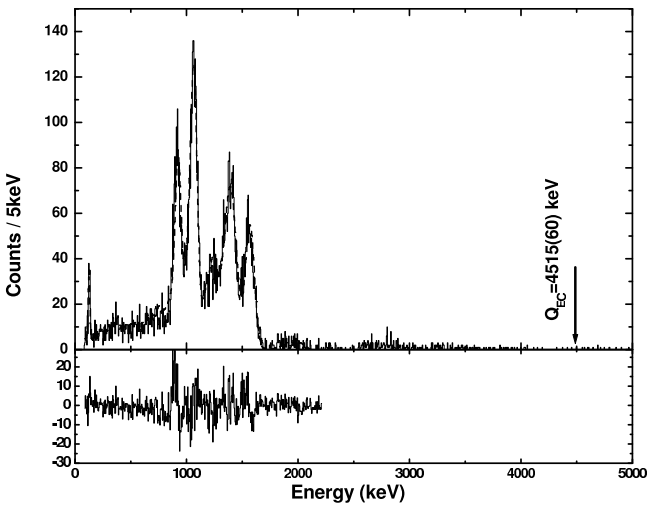

Fig. 2. Upper panel: TAS spectrum of the EC component of ^{104}Sn β decay (solid line) and corresponding simulated spectrum (dashed line). Lower panel: Difference between experimental and simulated spectra presented in upper panel. The range of the spectrum corresponds to the range of the fit.

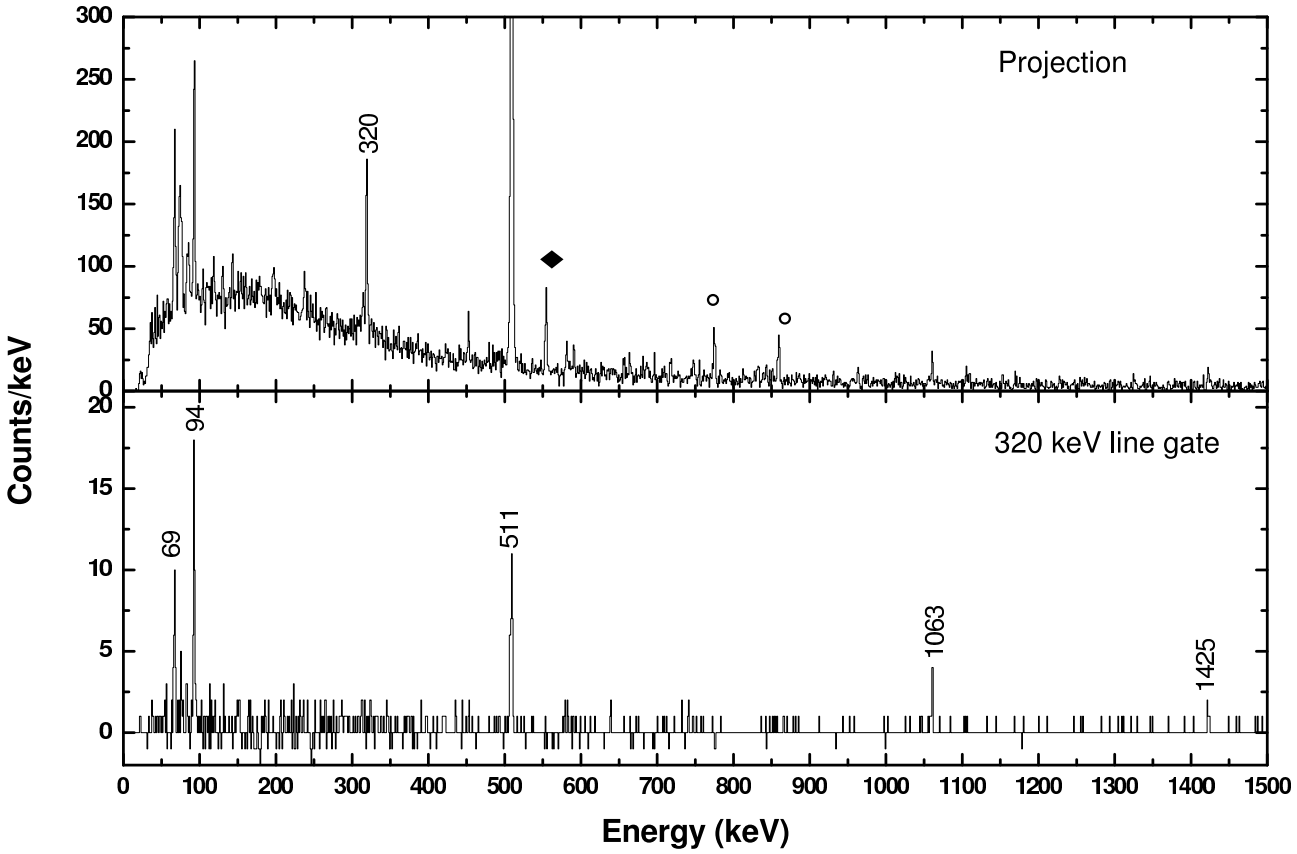

Fig. 3. Examples of γ-ray spectra obtained from the high-resolution data collected for the decay of ^{102}Sn. The upper panel shows data resulting from the total projection of the β-gated γ-γ matrix while the lower panel presents a spectrum obtained in coincidence with the 320 keV transition. The strong lines from isobaric contamination of ^{102}In and ^{102}Ag are marked by open circles and a full diamond, respectively. Lines marked by their energies in keV have been assigned to the decay of ^{102}Sn.

Figure 1 includes also the β intensities (I_β) derived from the TAS data and the corresponding comparative half-life values ($\log ft$). Due to the strong contamination of the positron-gated TAS spectra by isobaric indium and silver activities, the I_β values were determined by using the EC intensities (see below) and normalizing them by means of theoretical EC/total ratios [25]. In view of the poor energy resolution of TAS, we were unable to deduce I_β data for the 1634 and 1651 keV states individually. Therefore, the value of 26% (see fig. 1) has to be considered as the summed β-feeding to both levels. The I_β result of 0.5% for the 2072 keV level, indicated within parentheses in fig. 1, is positive but of the same order of magnitude as the experimental uncertainty ($\Delta I_\beta \approx 0.5\%$). Figure 2 presents the EC-related TAS spectrum together with the simulated spectrum and the difference between them. The double-peak structure occurring around 1000 keV in this spectrum corresponds to the de-excitation of a 1139 keV level which de-excites mainly to the (3^+) isomeric state at 93.5 keV. The high-energy component of the doublet at the energy of 1046 keV (1138.8 − 93.5 keV) is interpreted as representing events in which all γ-rays of the relevant cascade, except the isomeric 94 keV transition (see fig. 1) are detected by the main TAS crystal. In contrast, the low-energy component of the doublet at the energy of 913 keV (1139 − 93 − 133 keV) is mainly due to a de-excitation path in which the 133 keV γ transition is converted, leading to the emission of an electron of about 109 keV and In X-rays. Such low-energy electrons get absorbed in material in the center of the TAS (mainly Si detectors) and do not contribute to the total energy registered by TAS. In contrast, the X-rays from conversion are recorded by the Ge detector of TAS, thus increasing the probability of detecting the X-ray-TAS coincidence events (two X-rays per event instead of one) required for the EC spectrum increment. In the calculation of the simulated TAS spectrum, such a scenario was taken into account by introducing an internal conversion coefficient $\alpha_K = 0.22$ [24] for the 133 keV, $M1$ transition multiplied by 2. The above is also true for the 93.2 keV transition but due to the low intensity (only 5% of the β decays to the 1139 keV level proceeds via this transition) and the vicinity of 2 strong peaks this de-excitation path is not visible in fig. 2. The analysis of the TAS data did not yield any evidence for a significant β-feeding to the 1500 keV level. Therefore, this level is considered as tentative and no spin assignment is suggested. The distribution of β-feeding deduced in this work (see fig. 1) yields, together with a Q_{EC} value of 4515(60) keV [26] and the half-life 20.8(5) s [24], a B_{GT} value equal to 2.7(3).

Table 2. Energies E_γ, intensities (I_γ) and γ-γ coincidence relationships of β-delayed γ-rays assigned to the ^{102}Sn decay. The uncertainty of the γ-ray energies amounts to about 1 keV. The I_γ values, obtained in positron and 511 keV coincidence, were corrected for the energy-dependent photo-peak efficiency. The transition intensities may be different from I_γ due to electron conversion.

E_γ (keV)	I_γ [a]	Energies of γ-rays observed in coincidence (keV)
69	1.0(2)	94, 320, 511, 1063
94	0.9(2)	69, 87[b,c], 320, 511
238	0.25(10)	120[c], 511, 538,
320	1	69,77[c], 85[c], 94, 511, 581[b,c], 641[b,c], 1063, 1425
538	0.3(1)	69, 239, 511
583	0.4(1)	94, 511, 844
844	0.3(1)	94, 510, 583
1063	0.5(2)	69, 94, 144[b,c], 210[b,c], 320, 511
1107	0.3(1)	69, 94, 258[b,c], 511
1425	0.4(2)	94, 178[b,c], 320, 500[b,c], 511

[a] Normalized to the intensity of the 320 keV line.
[b] Very weak relationship.
[c] Not placed in the level scheme.

3.2 Beta decay of ^{102}Sn

The β decay of ^{102}Sn was recently studied by Stolz *et al.* [27,28] who used fragmentation reactions induced by a 1 GeV/nucleon beam of ^{112}Sn. They determined the half-life and Q_{EC} value to be 3.8(2) s and $5760 \pm 90 \pm 50$ keV, respectively, and identified eight γ-rays to belong to this decay. In our work we adopted these values as the latest and the most accurate. As the authors of the fragmentation experiment used only one clover detector they were unable to get γ-γ coincidence relationships. Nevertheless, with the help of shell model calculations as well as experimental γ energies and intensities they proposed a level scheme. In our work based on γ-γ coincidence data we extend and partly correct the level scheme proposed by Stolz *et al.* [27,28].

3.2.1 High-resolution results

The high granularity and efficiency of the Ge array used in our work, together with the larger source strength compared to Stolz *et al.* [27,28], allowed us to collect for the first time β-γ-γ coincidence data for the decay of ^{102}Sn. Figure 3 shows the projection of the β-gated γ-γ matrix as well as the result of using a 320 keV gate (background subtracted) on the matrix. Table 2 presents the γ-ray data obtained in this part of the experiment. Unfortunately, as already mentioned in sect. 2.2, a hardware β-γ-γ trigger had to be used. Therefore, the γ-ray intensities listed in table 2 are related to the positron component of the decay and do not include its EC part. Based on the new high-resolution data we are able to add two more levels and three new γ-rays to the ^{102}Sn β-decay scheme which is displayed in fig. 4. The 53 keV γ-ray and the corresponding 53 keV level [27,28] were removed from the decay scheme (for details see sect. 3.2.2).

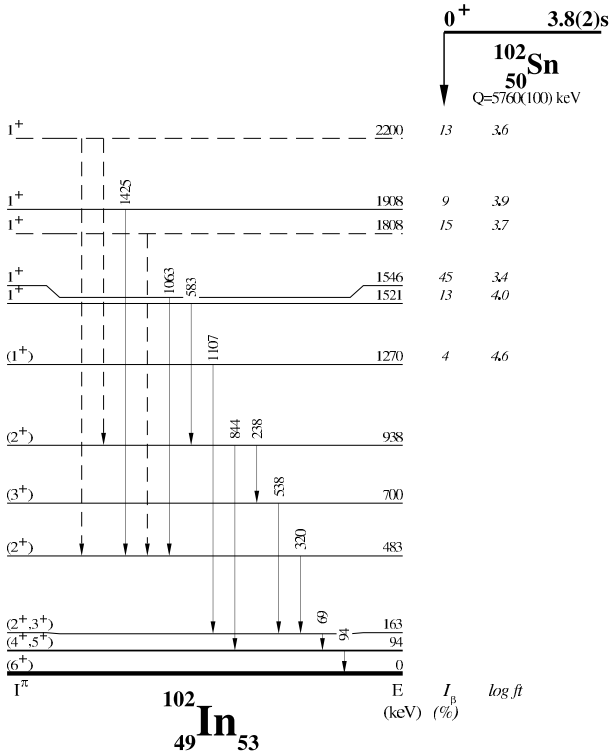

Fig. 4. ^{102}Sn decay scheme established in this work. The γ-ray energies and ^{102}In level energies marked by solid lines represent results from the high-resolution measurement, while dashed lines indicate levels and γ transitions added to the level scheme in order to reproduce the TAS spectrum. The β-feeding (I_β) and the comparative half-lives (log ft) stem from the TAS data.

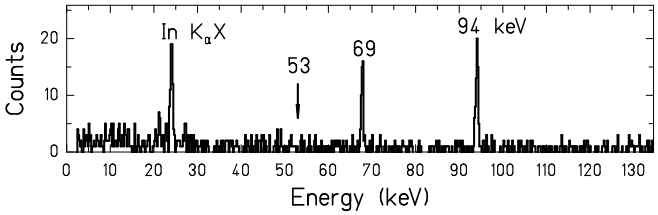

Fig. 5. Low-energy γ-ray spectrum obtained for the mass $A = 102 + 32$ by using the germanium detector of TAS. An arrow shows the expected position of the 53 keV line which remained unobserved in this experiment.

3.2.2 TAS results

The Ge detector of TAS (see sect. 2.3) can serve not only as a X-ray detector but also as low-energy γ-ray detector. Figure 5 shows the low-energy part of the spectrum obtained from this detector during the $A = 102 + 32$ measurement. This spectrum is characterized, besides the In X-rays, by two strong transitions of 69 and 94 keV which have already been observed in the Ge-Si data (see table 2).

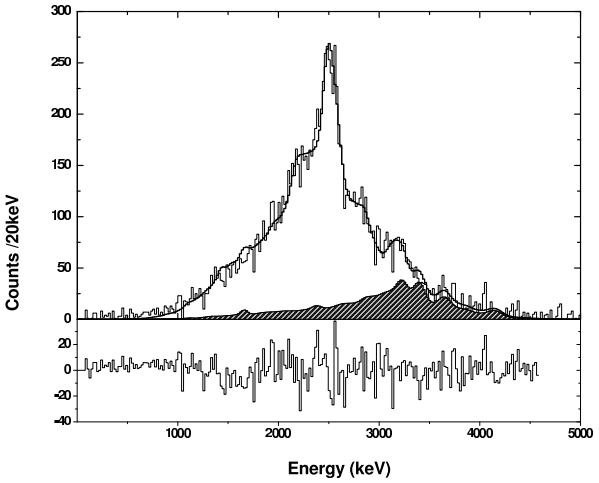

Fig. 6. Upper panel: experimental positron-coincident TAS spectrum of the β^+ decay of ^{102}Sn (histogram) and ^{102}Ag (hatched). The smooth thick line represents the result of a simulation based on the ^{102}Sn $\rightarrow$ ^{102}In decay scheme proposed in this work. Lower panel: difference between experimental and simulated spectra presented in upper panel. The range of the spectrum corresponds to the range of the fit.

However, there is no trace of the 53 keV line observed by Stolz *et al.* [27]. Therefore, the proposed level scheme shown in fig. 4 does not include a 53 keV transition in contrast to [27].

Due to its low statistics, the EC-related TAS spectrum obtained for ^{102}Sn could not be used for a reliable data analysis. Therefore, the evaluation of the TAS data obtained for the β decay of ^{102}Sn was restricted to the positron-decay spectrum displayed in fig. 6. As this spectrum was obtained by a simple coincidence between signals from the NaI crystals and the TOP or BOT detectors (see sect. 2.3), it may contain contributions from the decays of isobaric contaminants, *i.e.* mainly ^{102}In and ^{102}Ag. A simple subtraction of the long-lived activity of these contaminants, determined in separate measurements (see sect. 2.3) purified the positron-coincident TAS spectrum with respect to the entire ^{102}In and part of the ^{102}Ag contribution. The remaining ^{102}Ag activity was estimated by simulating the positron-coincident TAS spectrum of this nucleus. For this purpose we used the β-decay data from [29] as well as results obtained from previous GSI on-line mass separator experiments [30]. In this simulation, only the β-decay of the high-spin (5^+) isomer of ^{102}Ag was taken into account which is supposed to be dominantly produced in the heavy-ion fusion-evaporation reaction used in our work.

As already mentioned in sect. 3.1, in the case of highly converted β-delayed γ-rays one has to take corrections for electron conversion into account. The best fit, shown in fig. 6, was obtained by assuming $E2$ and $M1$ multipolarities for the 94 keV and 69 keV transitions, respectively (see fig. 4). This is in agrement with the multipolarity assignments made in [27,28]. Two "pseudo-levels" at 1808 keV and 2200 keV excitation energy were added to reconstruct ^{102}Sn decay experimental spectrum. The accuracy of the energy position of those levels is on the level of 40 keV and has a negligible influence on the total B_{GT} obtained. The assumed intensities of the γ-rays de-exciting "pseudo-levels" are below the sensitivity limits of the high-resolution setup used in this experiment.

The β^+-related intensities, obtained from the analysis of the TAS data, were divided by the theoretical β^+/total ratios [25] in order to obtain the total β intensities which are presented in fig. 4. These values were used to calculate a total GT strength of 4.2(8) for the decay of ^{102}Sn.

4 Discussion

4.1 ^{104}Sn

Although the measurement and the analysis of the β decay of ^{104}Sn were initially intended as a test of the unfolding method in the presence of highly converted γ-rays, the collected data extend the known level scheme. The new B_{GT} value of 2.7(3) is in agreement with that determined previously. This proves that small shifts in the β-feeding distribution have almost no effect on the B_{GT} value.

Spin and parity for the 1651 keV level in ^{104}In are suggested to be $J^\pi = 1^+$ on the basis of the non-zero feeding and the low $\log ft$ value as well as $J^\pi = 0^+$ assignment of the ground state in ^{104}Sn. Due to the large uncertainty of the β-feeding to the 2072 keV level we consider both the β-feeding and the spin/parity assignment (1^+) of this state as tentative.

4.2 ^{102}Sn

The ground-state spin of the ^{102}Sn even-even nucleus is 0^+. Therefore the strong β-feeding and the small $\log ft$ values for the 1521, 1546, 1808, 1908 and 2200 keV levels of ^{102}In lead us to assign $J^\pi = 1^+$ to them. In contrast, the (1^+) assignment of the 1270 keV state is tentative as its small β-feeding of 4% may include unidentified population by γ de-excitation of higher-lying levels. The systematics of ground-state spin and parity assignments for odd-odd indium isotopes as well as in-beam work [31] suggest a 6^+ assignment for the ^{102}In ground state. This is in contrast to the assignment suggested by Stolz *et al.* [27,28] who reported the observation of a 53 keV line. As shown in fig. 5 this transition is not present in our data, therefore we use the value of 6^+. This value is consistent with the ground-state spin and parity assignments found for ^{100}In [10] and ^{104}In [24].

On the basis of $M1$ and $E2$ multipolarity assignments for the 69 keV and 94 keV transitions (see sect. 3.2), the most probable spin/parity assignment for the 94 keV and 163 keV levels of ^{102}In are 4^+ and 3^+, respectively. Assignments of 5^+ and 2^+ for the two levels are also possible though less probable. In addition, the theoretical calculations, discussed below, place the first 2_1^+ state at 0.7 MeV making a 2^+ assignment for the 163 keV state even less probable. The tentative spin/parity values given in fig. 4

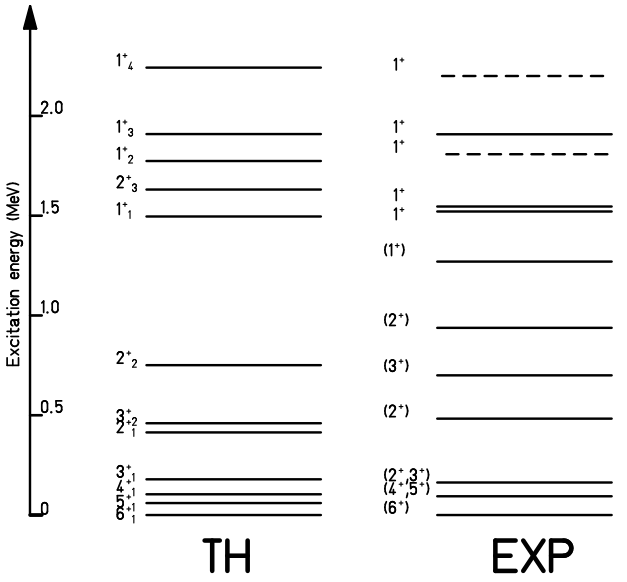

Fig. 7. Experimental (EXP) and calculated (TH) level energies and spin/parity assignments for ^{102}In. In the latter case, only the lowest-lying levels are displayed for spin values of 6, 5 and 4.

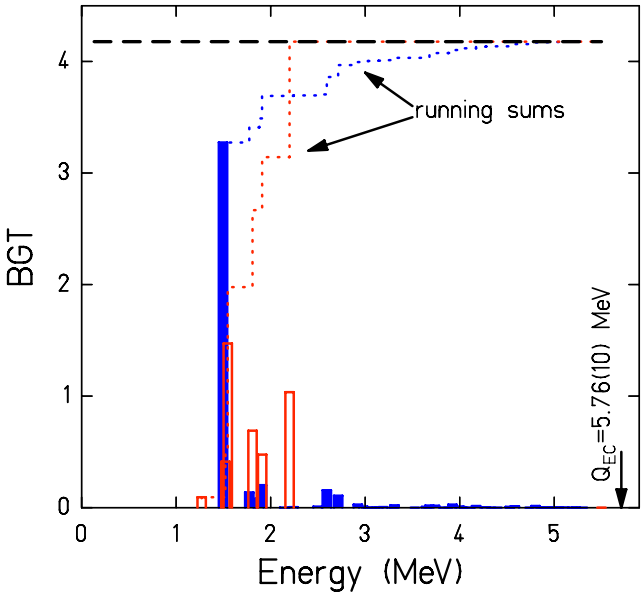

Fig. 8. (Color online) Theoretical (filled bars) and experimental (empty bars) Gamow-Teller strength function of the ^{102}Sn β-decay. The dotted lines show the corresponding "running sums". The theoretical calculations were scaled down by a hindrance factor of 3.6.

for the 483, 700 and 938 keV levels are based on the assumption that the depopulating transitions have dominantly $M1$ and $E2$ character and the excitation energies of these levels lie below the lowest-lying 1^+ and above the first excited $(4^+, 5^+)$ and $(2^+, 3^+)$ states.

Theoretical calculations of the β-decay of ^{102}Sn were performed within the $\pi(p_{1/2}, g_{9/2})^{11}$, $\nu(g_{7/2}, d_{5/2}d_{3/2}, s_{1/2}, h_{11/2})^3$ model space, using the SNC interaction [8, 32]. The SNC predictions are compared to the experimental data in fig. 7 with respect to properties of ^{102}In levels and in fig. 8 with respect to the GT strength. According to the shell model calculation with SNC interaction, most of the β-feeding (91%) goes to the 1^+ level at 1496 keV, which is very close in energy to two levels (1521 and 1564 keV) collecting 58% of the total β-feeding. This good agreement between this prediction and the experimental β-feeding observation confirms the very good predictive power of the SNC model concerning the localization of the GT-resonance (see also [7,8]). Although the SNC calculation predicts many (≈ 50) 1^+ states to occur within the Q_{EC} window, only the lowest-lying four levels of ^{102}In are expected to have a β-feeding above 1% while two additional 1^+ levels at 2.6 and 2.7 MeV get a β-feeding above 0.5%. Those six levels with a summed β intensity of 99.6% are predicted to exhaust 95% of the total B_{GT} strength of this decay (see fig. 8).

The systematics of low-lying states in ^{102}In, ^{104}In and ^{106}In, shown in fig. 9, reveal that the excitation energies of the 3_1^+ and 2_1^+ states increase with decreasing mass number, while the 4^+ state energies seems to decrease. The most important consequence of this observation is a gradual disappearance of the β-decaying isomer in light indium isotopes. In ^{106}In all γ cascades end at the 3^+ state at 28.6 keV while in ^{104}In already 10% of the γ

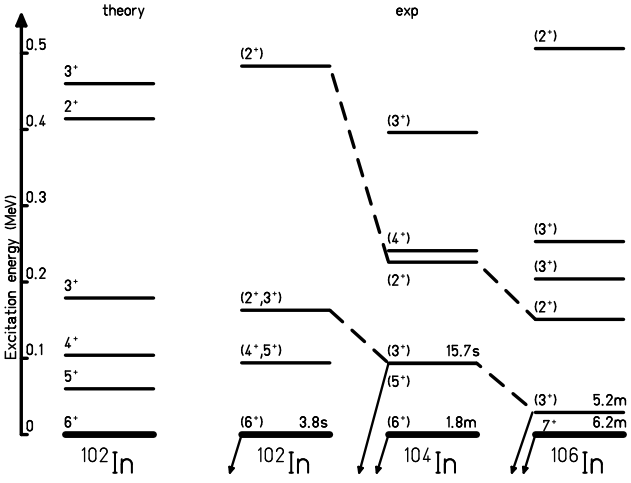

Fig. 9. Systematics of low-lying levels in even-even indium isotopes.

intensity bypasses the 3^+ isomeric state at 93.2 keV. In the case of ^{102}In, the data presented in this work indicate that β-delayed γ cascades populate the (6^+) ground state without yielding evidence for a (long-lived, β-decaying) isomer. This is in agreement with the non-observation of the β-decaying high-spin isomer in the β-decay studies of ^{102}In [11].

As the energy difference of 25 keV between the 1521 keV and 1546 keV levels is below the energy resolution of the TAS, the β-feedings deduced for the two levels may not be reliable. This possibility is also suggested by

the very low log ft value found for the 1564 keV level and the relatively high one deduced for the 1521 keV state. However, due to the small energy difference between the two levels, potential error due to incorrectly assigning partial β-feeding to them has a negligibly small influence on the B_{GT} value as long as the total β-feeding to the respective energy region remains unchanged.

The B_{GT} value of the ^{102}Sn β decay obtained in this work amounts to 4.2(8). Almost 70% of the uncertainty of this result is related to the Q_{EC} value which has an uncertainty of 100 keV. By deducing a hindrance factor defined as the ratio between predicted and experimental B_{GT} value and comparing this to the corresponding data of other isotopes in the vicinity of ^{100}Sn, one is able to test shell model calculations and to predict the total B_{GT} value for nuclei further away from stability, including ^{100}Sn. With the B_{GT} value of ^{102}Sn predicted by the SNC model to be 15.3, one gets a hindrance factor of 3.6(7) for this decay. This agrees with the values of 3.8(7) and 4.1(9) found for ^{98}Cd [32] and ^{100}In [10], respectively. The agreement between experimental and calculated positions of the most intensely fed 1^+ level for the presented ^{102}Sn case as well as for other isotopes from the vicinity of ^{100}Sn [6–8] indicates that the SNC model is able to reliably predict the position of the maximum of the GT strength function for nuclei close to ^{100}Sn. The SNC calculation shows that the 1^+ level in ^{100}In being fed in the β decay of ^{100}Sn with 100% intensity is located at the excitation energy of 1790 keV.

5 Summary

In this paper we presented results on the β-decay properties of ^{104}Sn and ^{102}Sn. By combining on-line mass separation with high-resolution and total absorption spectroscopy, the knowledge of the decay properties of the two nuclei was substantially improved, including the extension of the decay schemes and the determination of their total B_{GT} strength. The experimental data were discussed in comparison with predictions of the SNC model. The resulting hindrance factor of ^{102}Sn is in good agreement with those found previously for ^{98}Cd and ^{100}In, the two other members of the family of two-particle/hole nuclei southeast of ^{100}Sn.

The improvements of the decay data for ^{104}Sn and ^{102}Sn obtained in this work are due to the molecular-ion technique which leads to a considerable reduction of the isobaric contamination. However, this method reaches its limits in terms of intensity and purity of the mass-separated beams when extended to ^{101}Sn [14,33] and ^{100}Sn [14]. This is the reason why recent attempts at the GSI on-line separator to improve the β-decay data of ^{100}Sn have remained unsuccessful. All in all, such β-decay measurements, including those on the nearest one-neutron particle/one proton-hole neighbours of ^{100}Sn, ^{99}In and ^{101}Sn, may have to wait until the new radioactive beam facilities will become available.

The authors would like to thank K. Burkard and W. Hüller for their many valuable contributions to the development and operation of the GSI on-line mass separator. This work was supported in part by the Polish Committee for Scientific Research funds of 2004, under Contract No. 2P03B 035 23. B.A. Brown acknowledges support from NSF grant PHY-0244453. A. Jungclaus acknowledges support from the Spanish Ministerio de Educación y Ciencia within the Ramón y Cajal program.

References

1. K. Rykaczewski *et al.*, Z. Phys. A **322**, 263 (1985).
2. K. Rykaczewski *et al.*, Z. Phys. A **332**, 176 (1989).
3. H. Keller *et al.*, Z. Phys. A **339**, 355 (1991).
4. A. Płochocki *et al.*, Z. Phys. A **342**, 43 (1992).
5. L. Batist *et al.*, Z. Phys. A **351**, 149 (1995).
6. M. Karny *et al.*, Nucl. Phys. A **640**, 3 (1998).
7. Z. Hu *et al.*, Phys. Rev. C **60**, 024315 (1999).
8. Z. Hu *et al.*, Phys. Rev. C **62**, 064315 (2000).
9. M. Karny *et al.*, Nucl. Phys. A **690**, 367 (2001).
10. C. Plettner *et al.*, Phys. Rev. C **66**, 044319 (2002).
11. M. Gierlik *et al.*, Nucl. Phys. A **724**, 313 (2003).
12. M. Kavatsyuk *et al.*, Eur. Phys. J. A **25**, s01, 139 (2005).
13. O. Kavatsyuk *et al.*, Eur. Phys. J. A **25** 211 (2005).
14. M. Karny *et al.*, Eur. Phys. J. A **25**, s01, 135 (2005).
15. R. Kirchner, Nucl. Instrum. Methods A **234**, 224 (1985).
16. R. Kirchner, Nucl. Instrum. Methods B **204**, 179 (2003).
17. I. Mukha *et al.*, Phys. Rev. C **70**, 044311 (2004).
18. M. Karny *et al.*, Nucl. Instrum. Methods B **126**, (1997) 411.
19. D. Cano-Ott *et al.*, Nucl. Instrum. Methods A **430**, (1999) 333.
20. D. Cano-Ott, PhD Thesis, University of Valencia (2000).
21. E. Nacher *et al.*, Phys. Rev. Lett. **92**, 232501 (2004).
22. J. Blachot, Nucl. Data Sheets **64**, 1 (1991).
23. R. Barden *et al.*, Z. Phys. A **329**, 319 (1988).
24. J. Szerypo *et al.*, Nucl. Phys. A **507**, 357 (1990).
25. B.S. Dzelepov *et al.*, *Beta Process* (Nauka, Leningrad, 1972).
26. G. Audi *et al.*, Nucl. Phys. A **729**, 337 (2003).
27. A. Stolz *et al.*, PhD Thesis, Universität München (2001).
28. A. Stolz *et al.*, AIP Conf. Proc. **638**, 259 (2002).
29. B. Singh, Nucl. Data Sheets **81**, 1 (1997).
30. A. Płochocki *et al.*, in preparation.
31. D. Sohler *et al.*, Nucl. Phys. A **708**, 181 (2002).
32. B.A. Brown, K. Rykaczewski, Phys. Rev. C **50**, R2270 (1994).
33. O. Kavatsyuk *et al.*, 2005 GSI Annual Report; in preparation.